How the Expansion of the Universe Relates to Redshift and the Planck's Length

Hector Gerardo Flores[1] and Maria Isabel Gonçalves de Souza[2]

[1] *Universidad Nacional de Tucumán, Tucumán Province, Argentina.*
[2] *Universidade Federal de Campina Grande, Campina Grande, Paraíba, Brazil.*

E-mail: [1]hectorisabel2011@hotmail.com; [2]isa271938@hotmail.com

(Received: Apr 28, 2026; Revised: May 20, 2026; Accepted: June 12, 2026; Published: June 30, 2026)

Abstract We show that the Planck length expansion can be modeled as a function of the redshift z. In our previous RLC electrical model of a black hole and the early universe, we proposed that during black hole formation, the Planck length corresponds to $L_{\text{pg}} = 1.61 \times 10^{-35}$ m. As the black hole grows, the Planck length decreases until the black hole reaches its critical mass and disintegrates, at which point the Planck length attains its minimum value of $L_{\text{pg}} = 1.28 \times 10^{-54}$ m. Using electrical RC circuit charge models, we demonstrate that the expansion of the Planck length follows exponential relaxation laws analogous to the charging of a capacitor, parameterized by specific time constants (τ). This new approach provides a geometric and thermodynamic insight into the nature of dark energy and the Hubble tension problem.

Keywords: RLC electrical model; RC electrical model; cosmology; astronomy; astrophysics; background radiation; Hubble's law; Boltzmann's constant; dark energy; dark matter; black hole; Big Bang; cosmic inflation; early universe; quantum gravity.

I Introduction

Cosmological redshift is a fundamental concept in astrophysics and cosmology that describes the stretching of light waves as they travel through an expanding universe. It occurs due to the large-scale expansion of space itself, rather than the relative motion of individual astronomical objects. The magnitude of this shift is directly related to the scale factor of the universe and provides crucial information about cosmic evolution.

In standard cosmology, the cosmological redshift is mathematically expressed by the following set of fundamental equations:

$$z = \frac{\lambda_{\text{obsv}} - \lambda_{\text{emit}}}{\lambda_{\text{emit}}}, \qquad 1 + z = \frac{\lambda_{\text{obsv}}}{\lambda_{\text{emit}}} \tag{1}$$

$$z = \frac{f_{\text{emit}} - f_{\text{obsv}}}{f_{\text{obsv}}}, \qquad 1 + z = \frac{f_{\text{emit}}}{f_{\text{obsv}}} \tag{2}$$

where λ_{obsv} and f_{obsv} represent the wavelength and frequency measured by the observer, and λ_{emit} and f_{emit} are the wavelength and frequency at the time of emission. This relationship is linked to the scale factor via Hubble's Law:

$$v = H_0 \cdot d \tag{3}$$

where v is the recession velocity of a galaxy, H_0 is Hubble's constant, and d is the distance to the galaxy.

The standard Lambda CDM model, however, faces severe discrepancies when attempting to reconcile the value of the Hubble constant derived from the CMB (early universe) with that derived from local distance indicators such as Type Ia Supernovae (late universe). This work seeks to provide a novel theoretical bridge by modeling the fundamental Planck length as an expanding geometric object, relating its time evolution directly to the cosmological redshift.

II Cosmological Redshift Theory

The cosmological redshift is predominantly classified into three types:

1. **Doppler Redshift:** Due to the relative motion of sources moving away from an observer.
2. **Gravitational Redshift:** Caused by light escaping a strong gravitational field.
3. **Cosmological Redshift:** Resulting from the expansion of the universe itself, affecting all wavelengths of light traveling over vast cosmic distances.

In observational astronomy, the value of z is remarkably constant for distinct spectral lines from a single source. Distant objects may appear blurred or broadened due to thermal or mechanical motion, but the redshift remains accurately calculable. The true source of redshift allows us to reconstruct "lookback time", shown in Figure 1. Note that the furthest observation as of 2024 is the Lyman-break galaxy JADES-GS-z14-0 at $z = 14.32$, corresponding to 13.5 Gyr ago.

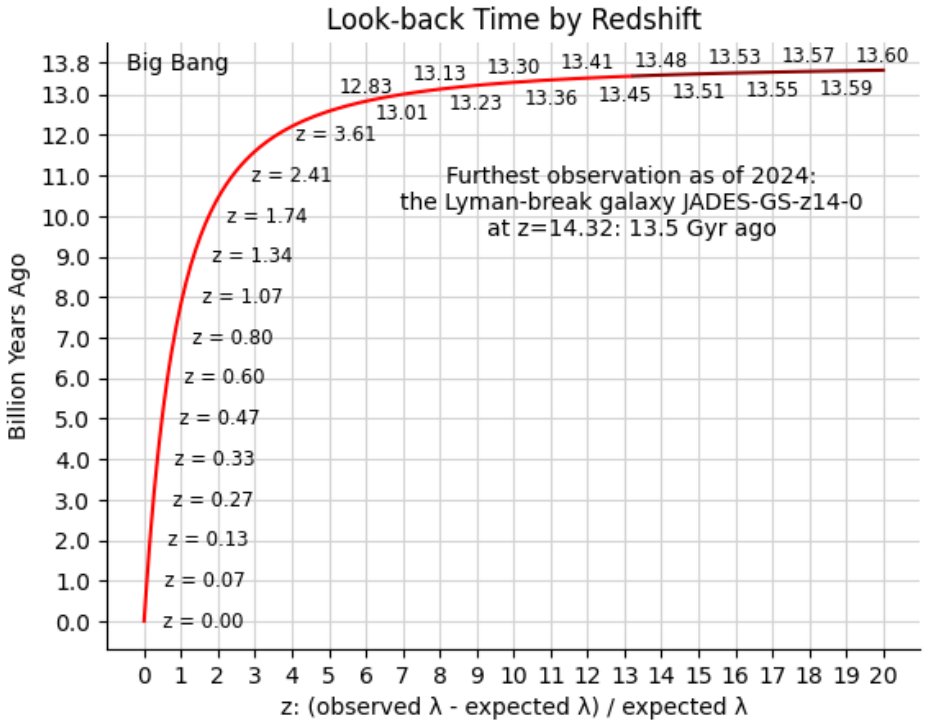


Figure 1: The standard lookback time of extragalactic observations by their redshift up to $z = 20$.

III Application of the Model and Results

The redshift observed in astronomy can be measured because the emission and absorption spectra for atoms are distinctive and well known, calibrated from spectroscopic experiments in laboratories on Earth. Determining the redshift of an object requires the wavelength of the emitted light in the rest frame of the source. Although gamma-ray bursts themselves cannot be reliably used for redshift measurements, their optical afterglows can be analyzed.

III.a RC Electrical Modelling of the Cosmological Redshift

To model the cosmological redshift, we utilize the capacitor charging curve of an RC circuit as shown in Figure 2.

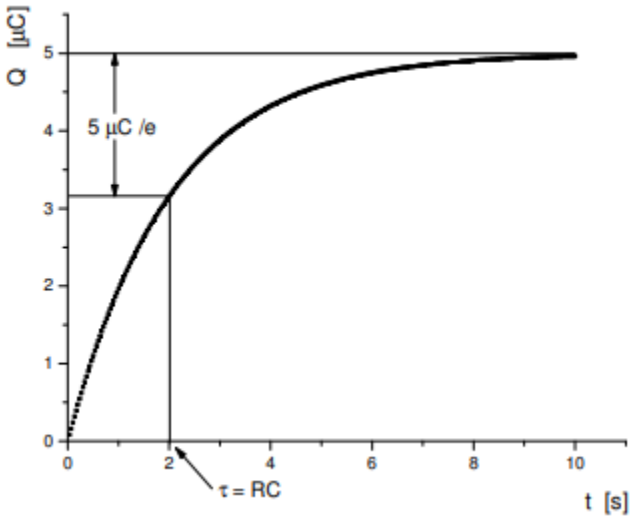


Figure 2: Charging process of a capacitor in an RC circuit.

The charge on the capacitor $Q(t)$ is described by the exponential equation:

$$Q(t) = C\epsilon\left(1 - e^{\frac{-t}{RC}}\right) \tag{4}$$

Here, C is the capacitance, ϵ is the electromotive force, and $RC = \tau$ is the time constant.

We map the lookback time (in billions of years) to the charge $Q(t)$, and the redshift z to the time t. Figure 3 shows the actual redshift curve (red) compared with two modeled capacitor charging curves (blue and green).

For the blue line, equation (4) is applied with $\tau = RC = 2$. For the green line, $\tau = RC = 3$. The blue line ($\tau = 2$) shows a significantly higher degree of alignment with the physical data (red line), indicating the time constant of the geometric expansion.

III.b Planck Length Analysis

We analyze the Schwarzschild solution for a point mass:

$$ds^2 = -\left(1 - \frac{2MG}{Rc^2}\right)c^2dt^2 + \left(1 - \frac{2MG}{Rc^2}\right)^{-1}dR^2 + R^2d\theta^2 + R^2\sin^2\theta d\phi^2 \tag{5}$$

where the Schwarzschild radius is $R_s = 2GM/c^2$.

Considering purely radial motion ($d\theta = d\phi = 0$) and analyzing the conditions inside a black hole ($R < R_s$, $v > c$), we find a space-type trajectory. We relate this to the Lorentz transformations for superluminal velocities:

$$L = iL_0\sqrt{\left(\frac{v}{c}\right)^2 - 1} \tag{6}$$

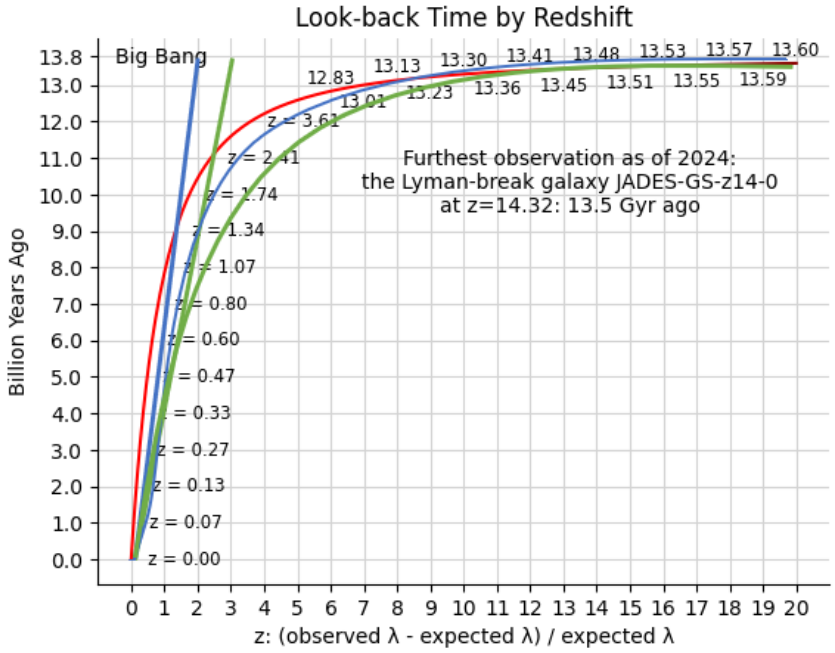


Figure 3: In blue and green, two RC models proposed to fit the redshift z (red).

where $L_0 = L_{\text{pe}} = 1.61 \times 10^{-35}$ m is the standard Planck length. As $v \gg c$, equation (6) dictates that the effective Planck length inside the black hole decreases. We therefore define an "electromagnetic Planck length", L_{pe}, and a "gravitational Planck length", L_{pg}, with $L_{\text{pg}} < L_{\text{pe}}$ always holding within a black hole.

III.b.1 The Spring Analogy

We hypothesize that the Planck length L_{pg} behaves like a compressed spring. As the black hole grows, L_{pg} decreases, accumulating immense gravitational potential energy. When the black hole reaches its critical mass and disintegrates, L_{pg} expands from 1.28×10^{-54} m (at time T_0^+) back to 1.61×10^{-35} m, releasing the stored energy as the exponential expansion of spacetime known as cosmic inflation.

III.c Variation of Planck Scales with Velocity

As established in equation (6), the speed of light inside a black hole can vary from $c = 3 \times 10^8$ m/s up to $c_g = 3 \times 10^{21}$ m/s, leading to extreme variations in the fundamental Planck scales (Table 1).

Table 1: Range of variation for the Planck length, time, and temperature inside a black hole.

Physical Constant	**Minimum Value**	**Maximum Value**
Velocity c_g	3×10^8 m/s	3×10^{21} m/s
Planck Length L_{pg}	1.28×10^{-54} m	1.61×10^{-35} m
Planck Time t_{pg}	0.42×10^{-75} s	5.39×10^{-44} s
Planck Temperature T_{pg}	1.41×10^{20} K	0.62×10^{90} K

Figure 4 illustrates the relationship between speed c_g and temperature inside the black hole, showing discrete transformations of spacetime state.

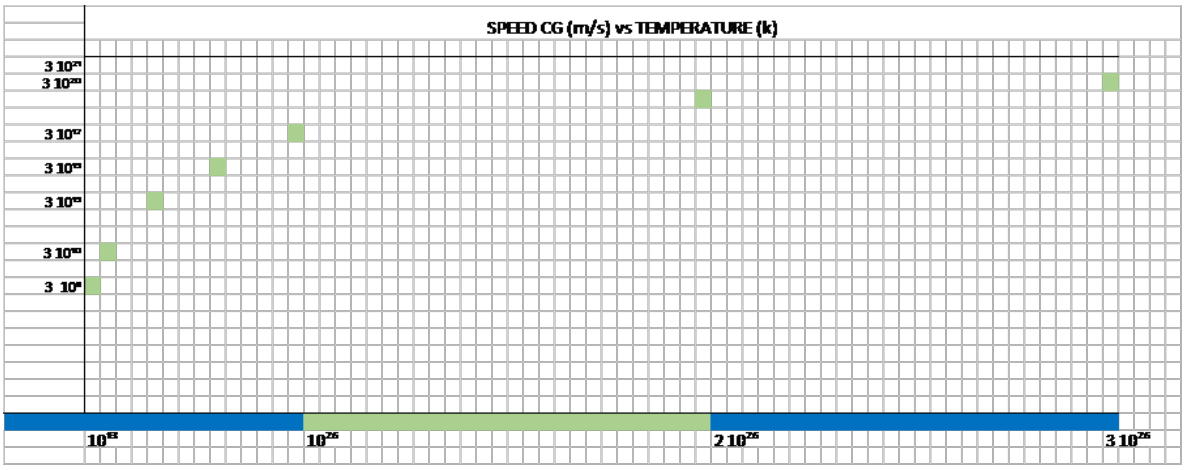


Figure 4: Variation of speed c_g (m/s) vs temperature (K) inside a black hole.

III.c.1 Physical Interpretation of the Imaginary Length

For $v > c$, the length equation takes the form $L = iL_0/\sqrt{(v/c)^2 - 1}$. The appearance of the imaginary unit i implies a geometric rotation: instead of continuing radially inward toward the singularity, the particle's trajectory deflects orthogonally by 90 degrees, adopting a circular motion analogous to the ergosphere of a Kerr black hole (Figure 5).

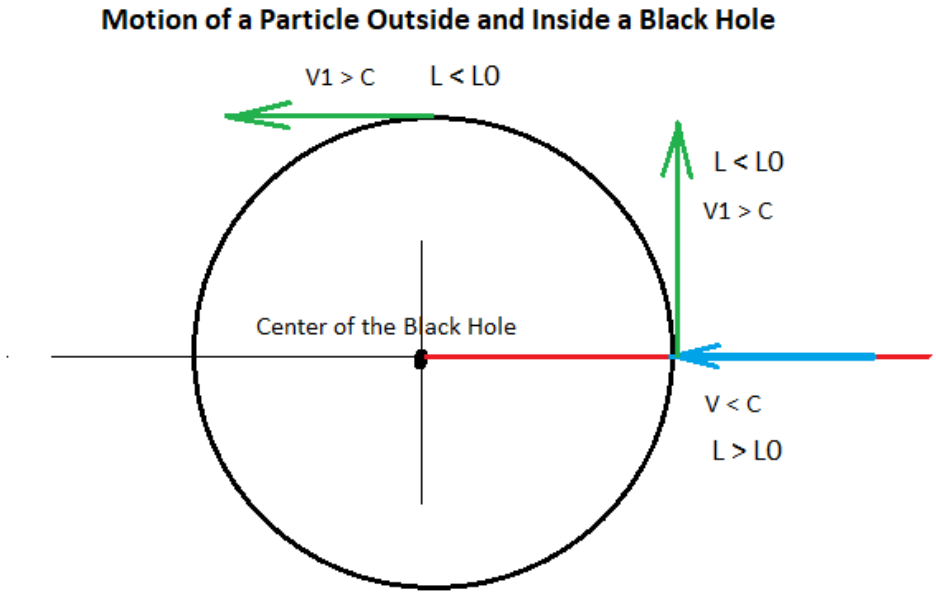


Figure 5: Motion of a particle outside and inside a black hole. The red line represents infall, while the green line shows the orthogonal rotational motion acquired inside the event horizon ($v > c$).

III.d Modelling Planck Length Expansion as a Function of Redshift

To build the model of Planck length expansion, we must first analyze the RLC electrical parameters which govern the gravitational wave spectrum of the early universe. The RLC circuit components are derived as follows:

$$
\begin{aligned}
R &= 3.60 \times 10^{51}\,\Omega, \\
L &= 1.98 \times 10^{62}\,\mathrm{H}, \\
C &= 1.26 \times 10^{-63}\,\mathrm{F}, \\
\omega_0 &= \frac{1}{\sqrt{LC}} \approx 2.00\,\mathrm{rad/s}, \\
\omega_1 &= -\frac{1}{2RC} + \sqrt{\left(\frac{1}{2RC}\right)^2 - \omega_0^2} \approx 1.81 \times 10^{-11}\,\mathrm{rad/s}, \\
\omega_2 &= \frac{1}{2RC} + \sqrt{\left(\frac{1}{2RC}\right)^2 - \omega_0^2} \approx 2.19 \times 10^{11}\,\mathrm{rad/s}
\end{aligned}
$$

The frequency spectrum produced in the inflationary phase (Figure 6) spans from ω_1 to ω_2 with bandwidth $B = 2.2 \times 10^{11}$ rad/s. The spacetime traverses a total of $e = 3.66 \times 10^{34}$ m, reaching stabilization at $t = 1.22 \times 10^{13}$ s.

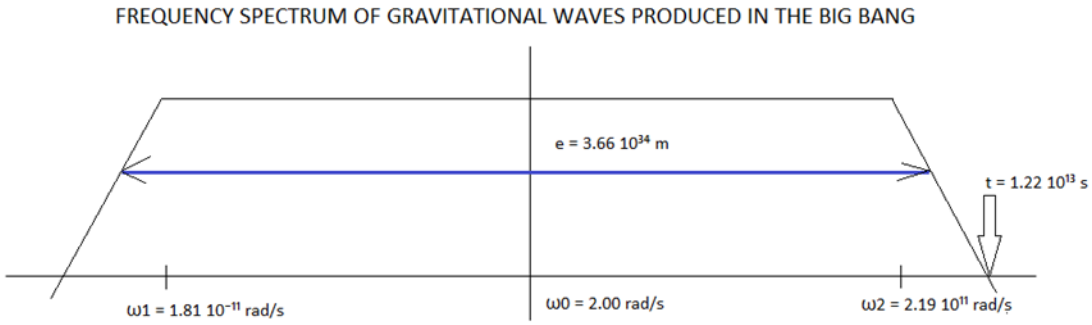


Figure 6: Spectrum of gravitational waves produced in the cosmic inflation.

III.d.1 Origin of Dark Energy

We identify two primary contributions to Dark Energy:

1. **Planck Length Spring Expansion:** At T_0^+, the Planck length $L_{\mathrm{pg}} = 1.28 \times 10^{-54}$ m expands toward its stable electromagnetic value $L_{\mathrm{pe}} = 1.61 \times 10^{-35}$ m at an initial velocity of 10^{21} m/s, generating the immense energy of inflation.
2. **Boltzmann's Constant Transition:** The Boltzmann constant shifts from $K_B = 1.78 \times 10^{-43}$ J/K (curved spacetime) to 1.38×10^{-23} J/K (flat spacetime). This transition causes the background gravitational waves to propagate at $c = 3 \times 10^8$ m/s, shaping the CMB power spectrum and determining the accelerated expansion of the universe.

Figure 7 displays the energy contribution of gravitational waves over time, showing a distinct cutoff at $t = 10^{26}$ s, while Figure 8 shows the Hubble parameter variation, indicating a transition from decelerated to accelerated expansion between $t = 10^{12}$ s and 10^{26} s.

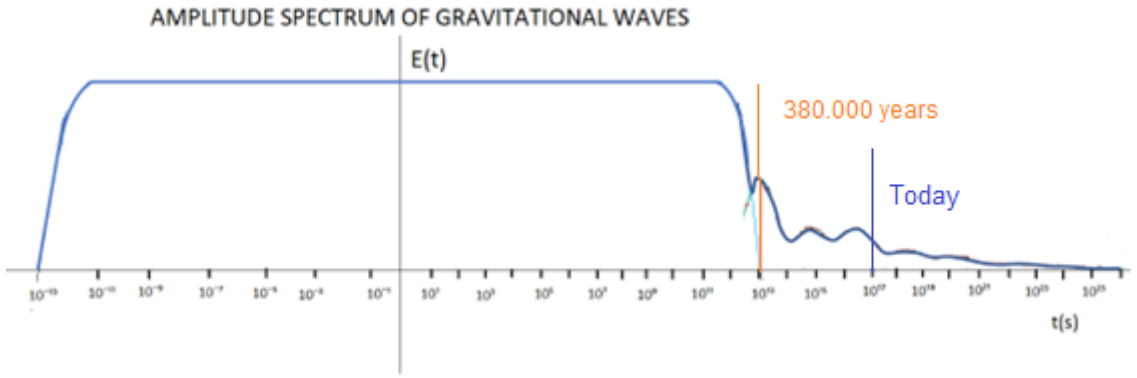


Figure 7: Energy contribution of gravitational waves versus time. At $t = 10^{26}$ s, the contribution becomes zero.

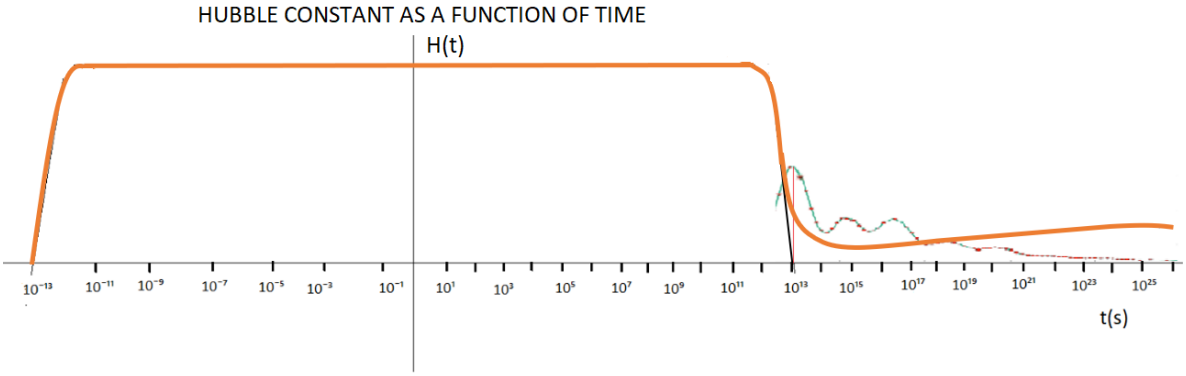


Figure 8: Variation of Hubble's constant versus time. The inflection point near 10^{12} s indicates the onset of accelerated expansion due to gravitational wave energy addition.

III.d.2 Reconciling the Hubble Tension

Measurements of H_0 vary based on the epoch being observed:

- Type 1A Supernova (local): $H = 74$ km/s/Mpc.
- CMB (early universe): $H = 67$ km/s/Mpc.
- Gravitational waves + EM: $H = 66.2$ km/s/Mpc.
- Type 1A Supernova + Gravitational lensing: $H = 64$ km/s/Mpc.

Our model solves this discrepancy by showing that the Hubble constant is not a universal invariant but a time-dependent function $H(t)$. The above measurements, taken at different cosmic epochs, inherently yield different values.

We further quantify the composition of the Universe using time-logarithmic mapping. Let $T_{\text{total}} = 10^{26}$ s (26 steps on a log scale). Today corresponds to $T_{\text{now}} = 4.35 \times 10^{17}$ s (17.5 steps).

$$\text{Dark Energy } \% = \frac{17.5}{26} \times 100 = 67.3\%$$
$$\text{Dark Matter } \% = 100\% - 67.3\% = 32.7\%$$

Similarly, using the time of recombination ($t = 11.81 \times 10^{12}$ s) and stabilization time ($t = 1.22 \times 10^{13}$ s):

$$\text{Baryonic Matter } \% = 100\% - \left(\frac{11.81 \times 10^{12}}{1.22 \times 10^{13}} \times 100 \right) = 3.28\%$$

Thus, the mass-energy content of the Universe at the time of CMB formation is found to be roughly: 67.3% Dark Energy, 29.42% Dark Matter, and 3.28% Baryonic Matter.

III.d.3 The Final Model: Planck Length vs Redshift

We propose three models using the capacitor charging equation $Q(z) = L_{\max}(1-e^{-z/\tau})$, where $L_{\max} = 12.8$ (representing steps in powers of 10 from 10^{-54} to 10^{-42}).

- **Model 1:** Lookback Time vs z with $\tau = 2$ (Blue line, Figure 9).
- **Model 2:** Lookback Time vs z with $\tau = 3$ (Green line, Figure 9).
- **Model 3:** Comoving Distance vs z with $\tau = 3.5$ (Figure 11).

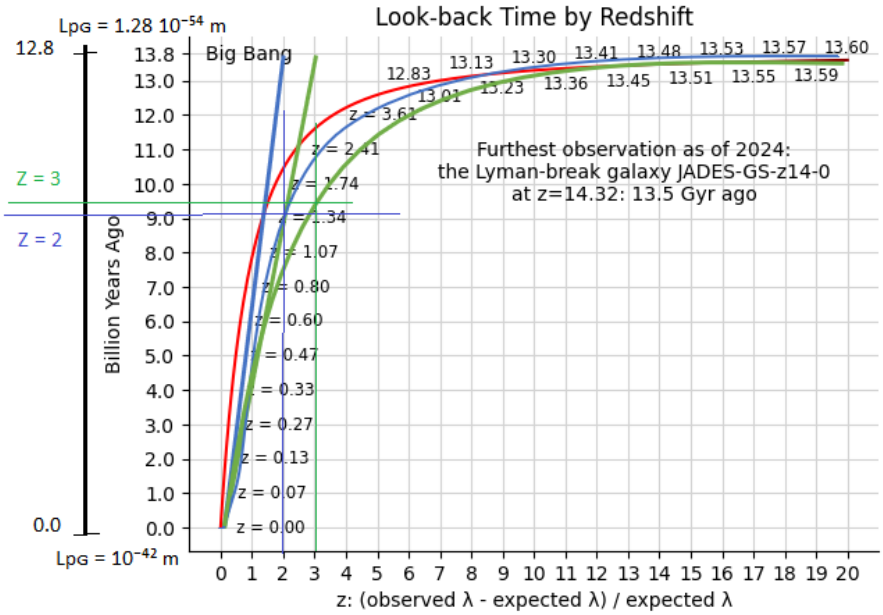


Figure 9: Lookback time vs Redshift modeling Planck length expansion. Blue line ($\tau = 2$), Green line ($\tau = 3$).

While the first two models provide approximate fits, Model 3 (using comoving distance, shown in Figures 10 and 11) is mathematically superior and more faithful to the perfect exponential charging curve of a capacitor.

Equation (7) defines the definitive relationship (Figure 12):

$$Q(z) = 12.80(1 - e^{-z/3.5}) \tag{7}$$

Applying this to $z = 3$: $Q(3) = 12.80 \times (1 - e^{-0.857}) \approx 8.8$, which corresponds to an equivalent Planck length scale of 10^{-50} m, aligning excellently with our theoretical predictions.

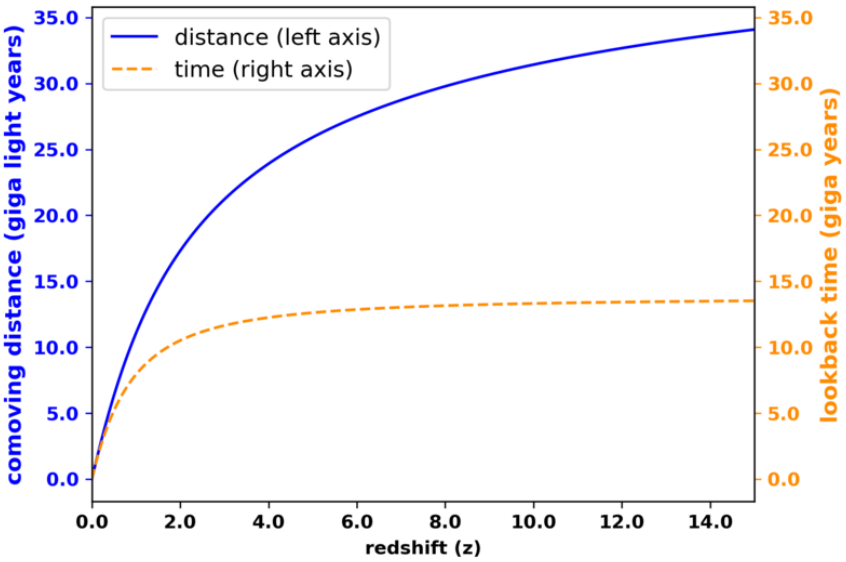


Figure 10: Comoving distance vs redshift z.

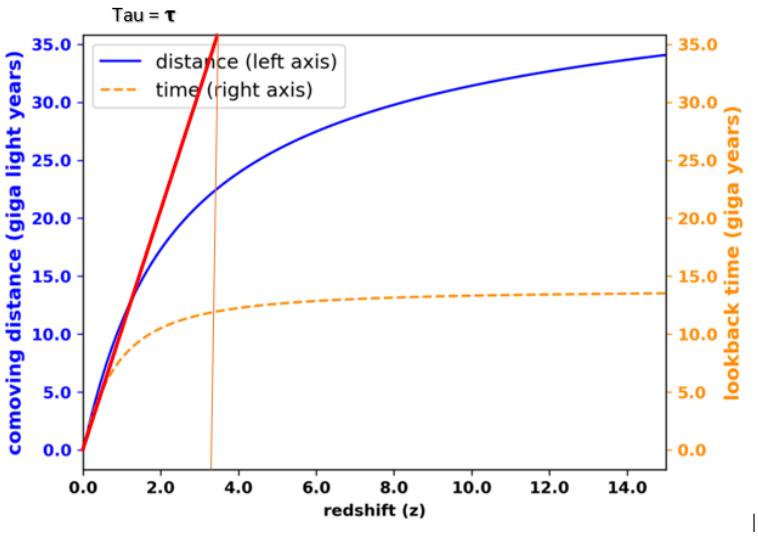


Figure 11: Modelling the comoving distance vs redshift using the capacitor charging curve.

IV Conclusions

We have demonstrated that the cosmological lookback time can be successfully modeled via the charge curve of an RC capacitor, providing a solid empirical fit for $\tau = 2$ and $\tau = 3$. Furthermore, the thermodynamic evolution of the Planck length inside a black hole—from $L_{\text{pg}} = 1.28 \times 10^{-54}$ m to $L_{\text{pe}} = 1.61 \times 10^{-35}$ m—was mapped directly onto the redshift z. We presented three phenomenological models based on this mapping. The final model, shown in Figure 12 (Equation (7)), uses comoving distance as the independent variable and yields a time constant $\tau = 3.5$. Our findings provide a consistent framework for understanding the origin of dark energy, the time-dependence of the Hubble constant, and the composition of the Universe (Dark Energy, Dark Matter, and Baryonic Matter).

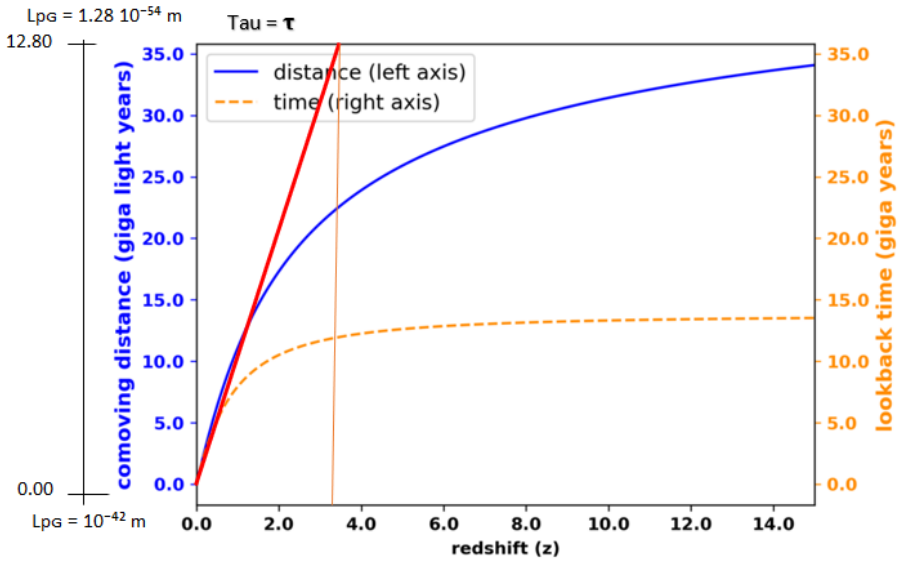


Figure 12: The true variation of the Planck length using Comoving Distance vs Redshift (z). The time constant is $\tau \approx 3.5$.

The expansion of the Planck length acts as a "spring" driving cosmic acceleration, effectively resolving the Hubble tension by showing that observations made at different cosmic epochs necessarily lead to different local measurements of H_0.

Acknowledgements

The authors thank the anonymous referees for their helpful suggestions.

References

[1] Xavier Calmet. Planck length and cosmology. *Modern Physics Letters A*, 22(25):1827–1835, 2007.

[2] Matthew Kleban, Mehrdad Mirbabayi, and Massimo Porrati. Effective planck mass and the scale of inflation. *Journal of Cosmology and Astroparticle Physics*, 2016(01):017, jan 2016.

[3] H. G. Flores. Rlc electrical modelling of black hole and early universe. generalization of boltzmann's constant in curved spacetime. *Journal of Modern Applied Physics*, 6(4):1–6, 2023.

[4] Hector Gerardo Flores and Maria Isabel Gonçalvez de Souza. The shannon-gibbs entropy and the effective boltzmann constant in curved space. *Natural Sciences and Applied Technology*, 3(1), March 2026.

[5] Kristjan Kannike, Gert Hutsi, Liberato Pizza, Antonio Racioppi, Martti Raidal, Alberto Salvio, and Alessandro Strumia. Dynamically induced planck scale and inflation. *Journal of Cosmology and Astroparticle Physics*, 2015.

[6] Ivan Arraut. The planck length as a duality of the cosmological constant: S-ds and s-ads thermodynamics from a single expression, 2012. Preprint.

[7] Circuito rc: Processo de carga e descarga de capacitores. Departamento de Física - ICE - UFJF. Course notes.

[8] Eleonora Di Valentino, Ankan Mukherjee, and Anjan A. Sen. Dark energy with phantom crossing and the h0 tension, 2024. Preprint.

[9] Hector Gerardo Flores and Maria Isabel Gonçalves de Souza. Black hole rc model: Calculating dark matter & galaxy rotation, March 2025. Preprint.

[10] H. G. Flores and M. I. Gonçalves de Souza. Theory of the generalization of the boltzmann's constant in curved space-time. shannon-boltzmann gibbs entropy relation and the effective boltzmann's constant, 2023. Preprint.

[11] H. G. Flores and M. I. Gonçalves de Souza. Rc electrical modelling of black hole. new method to calculate the amount of dark matter and the rotation speed curves in galaxies, 2023. Preprint.

[12] H. G. Flores, H. Jain, and M. I. Gonçalves de Souza. Origin of the dark energy, 2024. Preprint.

[13] H. G. Flores, H. Jain, P. Mahapatra, and M. I. Gonçalves de Souza. Analysis of the kerr-newman diagram. unravelling the interior of a black hole, 2024. Preprint.

[14] Espen Gaarder Haug and Gianfranco Spavieri. Micro black hole candidates and the planck scale. SSRN Preprint, 2024. Preprint.

[15] José F. Jesus, Mikael J. S. Gomes, Rodrigo F. L. Holanda, and Rafael C. Nunes. High-redshift cosmography with a possible cosmic distance duality relation violation, 2024. Preprint.

[16] Vahid Kamali and Mohammad Reza Setare. Tachyon-warm intermediate and logamediate inflation in the brane-world model in the light of planck data, 2015. Preprint.

[17] Francisco S. N. Lobo, José Pedro Mimoso, and Matt Visser. Cosmographic analysis of redshift drift, 2020. Preprint.

[18] Maysam Motaharfar and Hamid Reza Sepangi. Warm-tachyon gauss-bonnet inflation in the light of planck 2015 data, 2016. Preprint.

[19] Oliver H. E. Philcox, Soubhik Kumar, and J. Colin Hill. Too hot to handle: Searching for inflationary particle production in planck data, 2024. Preprint.

[20] Redshift. Wikipedia: The Free Encyclopedia. Accessed: 2026.

[21] Carlo Rovelli and Francesca Vidotto. Planck stars, white holes, remnants and planck-mass quasi-particles. the quantum gravity phase in black holes' evolution and its manifestations, 2024. Preprint.

[22] Noah Sailer, Emanuele Castorina, Simone Ferraro, and Martin White. Cosmology at high redshift – a probe of fundamental physics, 2021. Preprint.

[23] Laerte Sodré Jr. Cosmology with large redshift surveys, 2012. Preprint.

[24] Vincenzo Vitagliano, Jun-Qing Xia, Stefano Liberati, and Matteo Viel. High-redshift cosmography, 2009. Preprint.

Conflict of interest: The Authors have no conflicts of interest to declare that they are relevant to the content of this article.

About The License: © 2026 The Author(s). This work is licensed under a Creative Commons NonCommercial 4.0 International License (CC BY-NC 4.0) which permits unrestricted use, provided the original author and source are credited.